Synergistic Use of Lidar and Color Aerial Photography for Mapping Urban Parcel Imperviousness

Michael E. Hodgson, John R. Jensen, Jason A. Tullis, Kevin D. Riordan, and Clark M. Archer

Abstract

The imperviousness of land parcels was mapped and evaluated using high spatial resolution digitized color orthophotography and surface-cover height extracted from multiple-return lidar data. Maximum-likelihood classification, spectral clustering, and expert system approaches were used to extract the impervious information from the datasets. Classified pixels (or segments) were aggregated to parcels. The classification model based on the use of both the orthophotography and lidar-derived surface-cover height yielded impervious surface results for all parcels that were within 15 percent of reference data. The standard error for the rule-based per-pixel model was 7.15 percent with a maximum observed error of 18.94 percent. The maximum-likelihood per-pixel classification yielded a lower standard error of 6.62 percent with a maximum of 14.16 percent. The regression slope (i.e., 0.955) for the maximum-likelihood per-pixel model indicated a near perfect relationship between observed and predicted imperviousness. The additional effort of using a per-segment approach with a rule-based classification resulted in slightly better standard error (5.85 percent) and a near-perfect regression slope (1.016).

Introduction

Impervious surfaces such as concrete and asphalt pavement (and asphalt roof shingles) do not allow water to percolate through them. Instead, almost 100 percent of the incident precipitation runs off into the drainage network. Urbanization increases the amount of impervious surface, dramatically impacting hydrology, stream channel geomorphology, water chemistry, and biology (Paul and Meyer, 2001). Areas with a higher proportion of impervious surface will have increased discharge, decreased lag time to peak discharge, increased channel size, and decreased fish diversity. The percentage of the watershed that is impervious is one of the major variables required for accurately modeling rainfall runoff (Warwick and Tadepalli, 1991; Lohani *et al.*, 2002) and, subsequently, is a dominant parameter in water quality models (Zug *et al.*, 1999).

Numerous local, state, and federal regulations have attempted to limit the development of impervious surfaces by adjusting zoning regulations. At the local level, zoning changes for large parcels of land (e.g., commercial malls and residential developments) require an analysis of the modeled discharge changes before and after the proposed development. For example, county public works departments typically require a stormwater analysis to be performed prior to urban development (actually before zoning change approval) to estimate the additional discharge that will take place. This allows adequate retention basins and storm drains to be designed. Impervious surface information is critical for these calculations. Some local jurisdictions apply a stormwater levy (tax) based on the size and percentage of a parcel that is impervious (Kienegger, 1992). Consequently, an accurate representation of imperviousness is useful for planning, design, and economic factors. This article describes the extraction of imperviousness at the *parcel* level using high spatial resolution remotely sensed data and several digital image processing approaches.

Background

Considerable remote sensing research has focused on accurately mapping impervious surfaces. Most of the research has utilized statistical classification approaches (e.g., maximum-likelihood, clustering) with moderate spatial resolutions (e.g., 10 by 10 m to 30 by 30 m) from satellite imagery. Practically all previous work focused on multispectral imagery as the only input data source. We review some of the previous research approaches focused on imperviousness of surfaces that are particularly germane to the research presented here.

Coarse Spatial Resolution Remotely Sensed Data

Ridd (1995) evaluated the accuracy of mapping the fraction of impervious surface with Landsat Thematic Mapper (TM) 30-by 30-m multispectral imagery. Ji and Jensen (1999) mapped imperviousness from Landsat TM data using a subpixel classifier. In the Ji and Jensen study, percent imperviousness was classified into ten interval classes with overall classification accuracy at 83 percent. Wu and Murray (2002) used a linear spectral mixture model with Landsat 7 Enhanced Thematic Mapper Plus (ETM+) data to map impervious surface fractions. Phinn *et al.* (2002) mapped four land-cover categories (i.e., impervious, soil, vegetation, and water) from Landsat TM imagery with a resulting overall accuracy of only 45 percent. Sleavin *et al.* (2000) used Landsat TM imagery to map land-cover categories that were considered impervious and then determined parcel level imperviousness.

It is clear from such investigations that extracting detailed urban impervious surface information using relatively coarse

M.E. Hodgson, J.R. Jensen, J.A. Tullis and K.D. Riordan are with the Department of Geography, University of South Carolina, Columbia, SC 29208 (hodgsonm@sc.edu; jrjensen@sc.edu; tullis@gwm.sc.edu; riordank@mailbox.sc.edu).

C.M. Archer is with the Department of Public Works, Richland County South Carolina, Columbia, SC 29203 (rockyarcher@richlandonline.com).

Photogrammetric Engineering & Remote Sensing
Vol. 69, No. 9, September 2003, pp. 973–980.

0099-1112/03/6900–973$3.00/0

spatial resolution imagery and per-pixel classifiers is difficult. In addition, the 30- by 30-m spatial resolution associated with Landsat TM type data is insufficient for mapping imperviousness at the parcel level because the 900-m^2 pixel is greater than the physical dimension of many parcels.

High Spatial Resolution Remotely Sensed Data

The requirement for accurate impervious surface information at the *parcel* level is driven by the need to more effectively model the hydrologic system and to levy taxes on impermeable surfaces. For example, the City of Denver obtains its parcel level impervious surface information from the visual interpretation of panchromatic aerial photography (Kienegger, 1992). A stormwater surcharge for each owner is levied based on the parcel size and percent imperviousness.

Recently, automated techniques were applied to high spatial resolution digital imagery to map imperviousness. Fankhauser (1999) mapped impervious surfaces at the pixel level from high spatial resolution digital aerial photography (0.25 by 0.25 m to 0.75 by 0.75 m). He compared automated versus visually interpreted impervious surface classifications, aggregating the pixels to sub-catchments and catchment basins. Sub-catchment impervious surface errors were large while the imperviousness estimates for the catchment basins were within 10 percent of the reference data.

In addition to analog and digital aerial photography, there are two other sources of high spatial resolution information that will play an increasingly important role in the extraction of impervious surface information. Commercial satellite data providers such as Space Imaging, Inc. and DigitalGlobe, Inc. now provide panchromatic digital imagery with spatial resolutions from 1 by 1 m to 0.61 by 0.61 m, respectively. Light Detection and Ranging (lidar) imagery can now be obtained over entire states at very high spatial resolution (e.g., postings less than 1 m to 5 m). Multiple-return lidar data may provide vegetation height information to within $\pm$20 cm of its true height that may be of significant value for extracting impervious surface information (North Carolina Flood Plain Mapping Program, The State of North Carolina, Raleigh, North Carolina, URL: http://www.ncfloodmaps.com, date last accessed 16 September 2002).

Rule-Based and Neural Network Digital Image Processing

A considerable amount of research in the last 20 years has focused on the development of two non-statistical approaches to land-cover classification—Knowledge Based Expert Systems (KBESs) and Artificial Neural Networks (ANNs). An advantage of either of these approaches over per-pixel maximum-likelihood classification and spectral clustering is their applicability to use non-parametric data. Many land-cover classes exhibit skewed spectral distributions and, thus, are not ideal candidates for parametric statistical classification. In addition, many KBES and ANN approaches allow the use of nominal and ordinal data.

Civco *et al.* (2000) used an ANN approach for mapping sub-pixel (i.e., Landsat TM imagery) imperviousness with digital photography. Landsat imagery from two different seasons were used to map land cover and then were spatially distributed using the 2- by 2-m spatial resolution digital photography.

Numerous works have demonstrated the relative merits of these approaches. Practically all KBES classifiers use a rule-based classification model. The most difficult task within a rule-based model is building the rules. The common approaches for rule-base generation are (1) explicitly eliciting knowledge and rules from experts and then refining the rules (Stow *et al.*, 2003) (2) implicitly extracting variables and rules using cognitive methods (Hodgson, 1998; Lloyd *et al.*, 2002), and (3) empirically generating rules from observed data and automatic induction methods (Tullis and Jensen, 2003). Of the approaches for rule generation, the automatic induction method has generated increasing interest because the level of effort is relatively low and performance is reasonable.

Error Propagation when Mapping Imperviousness

If the overall accuracy of all observations in a classification is *x*-percent then the use of this classification product to produce another product typically results in an accuracy less than *x-percent*. The concept of decreasing accuracy is a basic tenent in error propagation and Bayesian methods of error accumulation. While this concept of error propagation is certainly true for many Bayesian modeling efforts, it is typically not valid for applications that merely *aggregate* data to a coarser scale. When aggregating data, errors of different signs (positive and negative) tend to cancel one another and the result is often more accurate than the individual unit of analysis (e.g., pixels). This advantage of scaling has been documented in statistical studies where the correlation coefficient between two variables increases with aggregation level (Clark and Avery, 1976). This aggregation benefit can be observed in geographic space (e.g., aggregation of pixels to census tracts) or measurement space (aggregation of ten classes to just five classes). For example, Fankhauser (1999) found that the accuracy of the impervious data aggregated to the catchment basin level was greater than impervious data disaggregated at the sub-catchment level. Based on this error propagation logic, the goal of this study was to accurately map the percentage of impervious surface at the parcel level (e.g., a parcel may be 1,000 m^2) using an aggregation of remotely sensed impervious surface information obtained at the pixel level (e.g., less than 1 by 1 m). Richland County, South Carolina Public Works engineering personnel suggest that $\leq$15 percent impervious surface mapping error is acceptable at the parcel level. The goal was to research remote-sensing-assisted procedures that could achieve this criterion. An important remotely sensed input source examined was surface cover height derived from multiple return lidar.

Methodology

Study Area

The study area was a 19.8-km^2 region in northwest Richland County, South Carolina (Plate 1). It consists of rolling piedmont terrain covered with dense, mixed deciduous and coniferous vegetation, and sprawling residential and commercial development. The study area did not include heavy industry or a central business district. Over the last ten years this area was part of the fastest growing region in Richland County. Most of the parcels in the study area were relatively small (less than 0.20 ha; 0.5 acre). Sixty parcels were selected and used as a reference dataset, ranging from 0.06 to 1.48 ha with an average size of 0.13 ha. The reference parcels were selected using a stratified random sampling design based on size classes.

Natural Color Aerial Photography and Lidar Data Collection

Natural color aerial photography and lidar data were collected for Richland County from 01 to 22 March, 2000 at a nominal height of 1,200 m (3,900 ft) above ground level (AGL). The color photography was scanned, orthorectified to a 0.3- by 0.3-m (1- by 1-ft) nominal spatial resolution, and color-balanced.

Lidar data were collected at a nominal 2- by 2-m posting using an Optech Airborne Laser Terrain Mapper (ALTM) 1210 system. The accuracy of the lidar postings ranged from a 17-cm RMSE in paved areas to a 26-cm RMSE in deciduous forests (Hodgson and Bresnahan, in press). Each lidar pulse

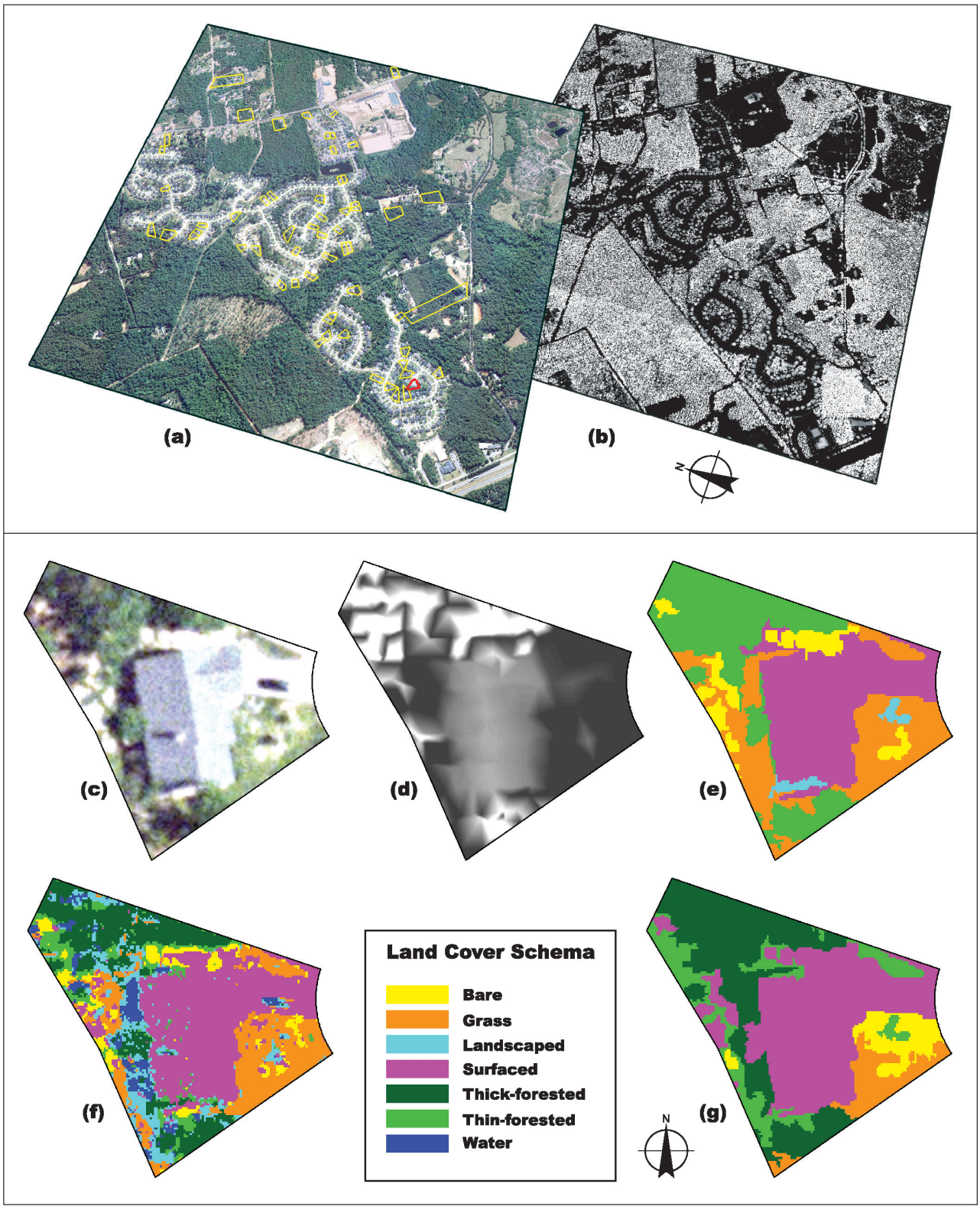

Plate 1. The natural color orthophotography of the study area in Richland County, South Carolina showing the 60 random parcels with an example parcel highlighted in red (a). Lidar-derived cover-height information (b). The same example parcel illustrating the quality of the digitized natural color orthophotography (c) and lidar-derived cover height (d). Reference land-cover map derived from visual classification of the orthophotography (e). Results of the maximum-likelihood pixel-level land-cover classification (f) and See5 rule-based segment-level classification (g).

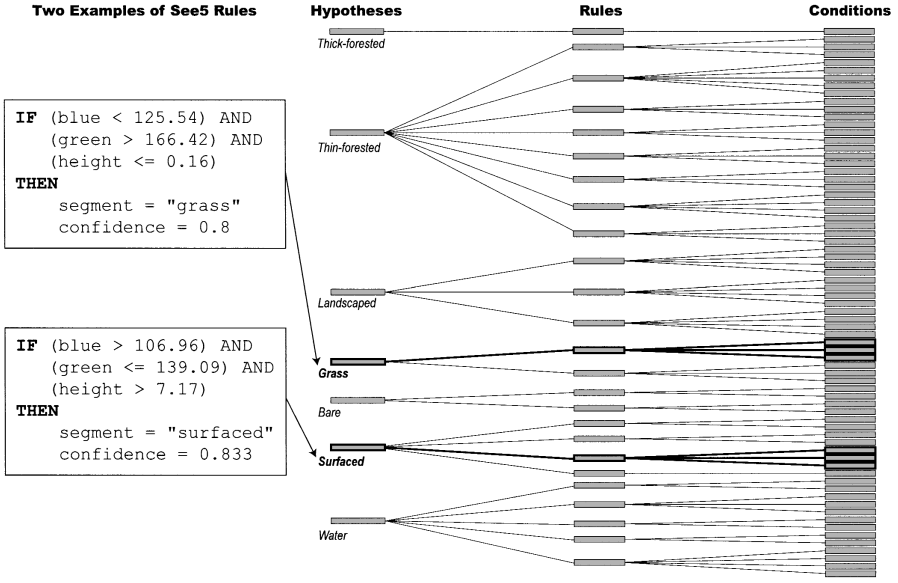

Figure 1. Two examples of the 25 See5 rules used to classify image *segments* into the seven imperviousness categories. Multiple conditions within a rule are separated by "AND" logic. Any rule evaluating to *true* causes the hypothesis to be *true*. If no hypotheses evaluate to *true,* the observation is classified as the category with the highest number of training samples.

was processed and labeled as "first return" or "last return." These data were then post-processed using spatial operators and human interpretation to produce "ground returns" that represented the "bald earth." In addition, the contractor provided a dataset of "first vegetation returns" that were interpreted as "vegetation canopy" (or possibly other above surface features).

A triangulated irregular network (TIN) was created for each of the lidar datasets—ground and surface cover. Digital surface models (DSMs) representing the ground and cover were then created from the respective TINs. The ground DEM was subtracted from the surface DEM to create the surface *cover height* model.

Classification Treatments

The three color channels from the aerial photography, together with the surface-cover height model, were processed using several techniques to derive the land cover of (1) each pixel and/or (2) the land cover for homogeneous segments within the imagery (Plate 1). Per-pixel classification was performed using (1) a maximum-likelihood algorithm, (2) an ISODATA clustering algorithm, and (3) See5-generated rules. Segment-level classification was performed using See5-generated rules. These algorithms were applied to natural color digital imagery, surface cover height data, and a combination of natural color digital imagery and surface height. Training regions (406) used in all classification approaches were based on the boundaries defined by the image segmentation process (discussed below). This allowed the same training areas to be used for both pixel-level and segment-level supervised classification and thus provided a controlled input for algorithm comparison. The same photointerpretation logic used to label training areas from image segments was used in labeling ISODATA clusters.

The See5 (release 1.13) inductive machine learning program (RuleQuest Research, 2001) was used to automatically generate production rules for the per-pixel and per-segment knowledge-based classifications. See5 is considered faster and more accurate (Data Mining Tools See5 and C5.0, RuleQuest Research, St. Ives, NSW, Australia, URL: http://www.rulequest.com/see5-info.html, date last accessed 18 April 2003) than its well-known predecessor C4.5 (Quinlan, 1993). The See5 program searches for an accurate decision tree to predict an array of training cases. The decision tree is simplified and converted to production rules where each rule (Figure 1) is composed of one or more *if-then* statements. Each rule is composed of one or more conditions, all of which must be met for the rule to be evaluated as true. Each rule also assigns a confidence level to the tentative land-cover label. Competing hypotheses are evaluated based on the sum of their rule confidences.

Although not designed specifically for image processing, the freely available C4.5 algorithm has been incorporated into a number of commercial data mining programs (e.g., aXi DecisionTree component by Neusciences, Hampshire, United Kingdom, URL: http://www.neusciences.com, date last accessed 15 April 2003) and has been shown to be a powerful non-parametric classifier when used with combined Landsat TM and ancillary GIS data (Huang and Jensen, 1997). More recently, Tullis and Jensen (2003) used See5 for automated house detection using size, shape, and contextual information in Ikonos imagery. This research used See5 in a manner similar to that of Tullis and Jensen (2003).

An increase in the number of training cases resulted in an even bigger increase in the number of rules and conditions within the knowledge base. When the combined color and cover height information were used as input data, only 25 unique rules (Figure 1) were generated from the 406 segment training cases, while 4,472 rules were generated from the 32,146 pixel training cases. Although the rule-generation process was completely automatic, the time required for generating the rules was considerable for the per-pixel classification. An inference engine was created using custom Avenue scripts in ArcView 3.2 to perform the actual per-pixel and per-segment land-cover classifications with the See5 generated production rules.

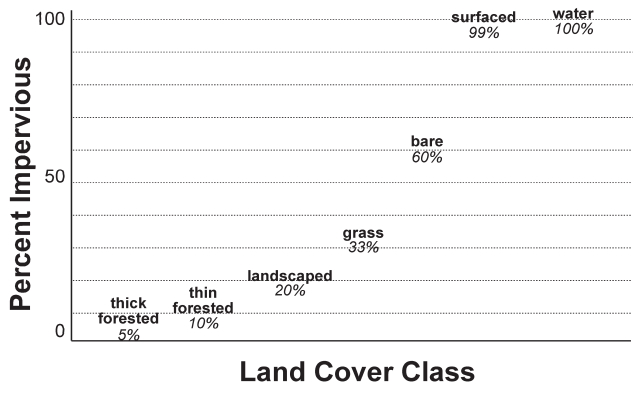

Figure 2. Percent imperviousness scale and land-cover categories.

Similar spectral/spatial image segments were automatically identified using eCognition software release 2.1. This method identifies contiguous, homogeneous pixels that have similar spectral responses and subsequently groups these similar pixels into segments (Definiens, 2002). By using this method, the 36.4 million pixels in the entire study area were reduced to 52,659 image segments. One benefit of this method is the reduction of the "salt-and-pepper" appearance that often occurs with pixel-level classifications. In the segment-level classification treatments the 52,659 segments were used in the image classification in place of the individual pixels. Each segment was classified using the See5 rule-based approach in a manner similar to that of the pixel-level rule-based classification. The mean multispectral values or mean cover height for each segment were used. While a host of other parameters are available as descriptors of image segments (e.g., perimeter-area ratio, mean value of neighboring segments, etc.), the parameters used in this research provide input control for comparison between pixel-level and segment-level objects.

Percent imperviousness for each parcel was mapped using the following two-stage logic. First, each pixel or segment was classified into one of seven major land-cover categories (Figure 2). Each of these land-cover categories was then associated with an average percent imperviousness, ranging from 0 to 100 percent. In theory, the "water" land-cover class might be given a value anywhere from 100 percent impervious (no ground infiltration) to 0 percent impervious (complete ground infiltration). Based on a worst-case rainfall effect, we considered water bodies as 100 percent impervious with all rainfall running off the surface.

The second stage was to compute the average percent imperviousness for each *parcel* of land. The boundaries of each parcel were available in digital format for the entire study area. First, the percent imperviousness of the land-cover class was assigned to each pixel (or segment). Second, the mean-area-weighted imperviousness of all pixels (or segments) within the parcel was summarized using a zonal cartographic modeling operation: i.e.,

$$I = \frac{\sum_{1}^{N} (A \times i)}{\sum_{1}^{N} A} \quad (1)$$

where I is the percent imperviousness of a parcel, N is the number of pixel centroids within (or segments intersecting) the parcel, A is the area of the pixel (or segment) within the parcel, and i is the percent imperviousness of the pixel (or segment).

Reference Data

Reference data were created from visual interpretation of the digital color aerial photography. For efficiency reasons, very small "segments" of the imagery were classified rather than individual pixels (Plate 1). The small image segments were created using the eCognition software. Both the natural color photography and the cover-height surface were used as input for the eCognition segment identification process. By overlaying the segment boundaries on the natural color photography, the land cover of each segment could be reliably identified and labeled. In a few instances the automatically generated segments contained more than one land-cover type. The interpreter would split these into individual segments and label them accordingly.

Statistical Analysis

Performance was assessed by comparing the results of various linear regression analyses of the predicted parcel-level impervious surface to reference impervious surface. The ideal regression line would pass through the origin and have a slope of 1.0. Significance tests for the regression slope were conducted. For all subsequent regression analyses the *y*-intercept was forced to 0.0. Mean standard error (in percent imperviousness) and the maximum error from the 60 parcels were also investigated.

Results

The research questions explored were

- Is there **additional information** in the lidar-derived cover-height data that is useful for impervious surface mapping?
- Which **classification methods** result in a more accurate estimate of imperviousness at the parcel scale?

The two data sources evaluated in this study were (1) digitized natural color orthophotography, and (2) a cover-height surface produced from multiple-return lidar data. A per-pixel classification approach was conducted using the following three classifiers:

- maximum-likelihood,
- ISODATA spectral clustering, and
- rule-based classification from using the See5 algorithm.

In addition, the See5 rule-based classification approach was performed on a per-segment level.

It was expected that the addition of lidar-derived cover-height information would result in a significantly higher accuracy than using just digital color orthophotography. In most instances, the land cover is vegetation and we expected the height information to help in shadowed areas and in separating short vegetation (i.e., grassland and landscaped) from tall vegetation (e.g., forests). Because of the non-normal distribution of the lidar height information, we expected the non-parametric rule-based approach to perform better than either the maximum-likelihood or spectral clustering approaches. Also, because of spectral overlap in the high spatial resolution remote sensor data, we expected the aggregate segment-level rule-based classification to outperform the pixel-level rule-based classification.

Relative Contribution of Lidar Data

The addition of the lidar-derived cover-height information improved the modeled imperviousness results for *all* classification approaches (Table 1). R^2 values increased by 2 percent (rule-based pixel classification) to 25 percent (clustering approach). The standard error for all classification approaches when using both the color imagery and the cover height was lower than when using any single data type. The additional information in the cover-height data is apparent when examining the bivariate plots of modeled imperviousness and reference imperviousness (Figure 3). For the parcels with low

TABLE 1. STATISTICAL ANALYSIS BETWEEN REFERENCE AND MODELED PERCENT IMPERVIOUS SURFACE (*y*-INTERCEPT FORCED THROUGH ORIGIN)

Classification Model	Data	R^2	Regression Line Slope	Maximum Residual (Percent Imperviousness)	Standard Error (Percent Imperviousness)
Per-Pixel					
Maximum-Likelihood	Color	0.66	0.923	−17.97	7.20
	Lidar	0.40	1.370	−27.65	9.57
	Both	0.71	0.955	**14.16**	6.62
ISODATA	Color	0.27	0.789	−38.60	10.52
	Lidar	0.51	0.945	−22.60	8.65
	Both	0.52	0.938	−22.41	8.56
See5 Rule-Based	Color	0.64	0.695	−17.25	7.42
	Lidar	0.46	1.650	−26.88	9.06
	Both	0.66	0.709	−18.94	7.15
Per-Segment					
See5 Rule-Based	Color	0.61	0.920	19.93	7.75
	Lidar	0.22	1.310	−27.71	13.65
	Both	**0.78**	**1.016**	14.85	**5.85**

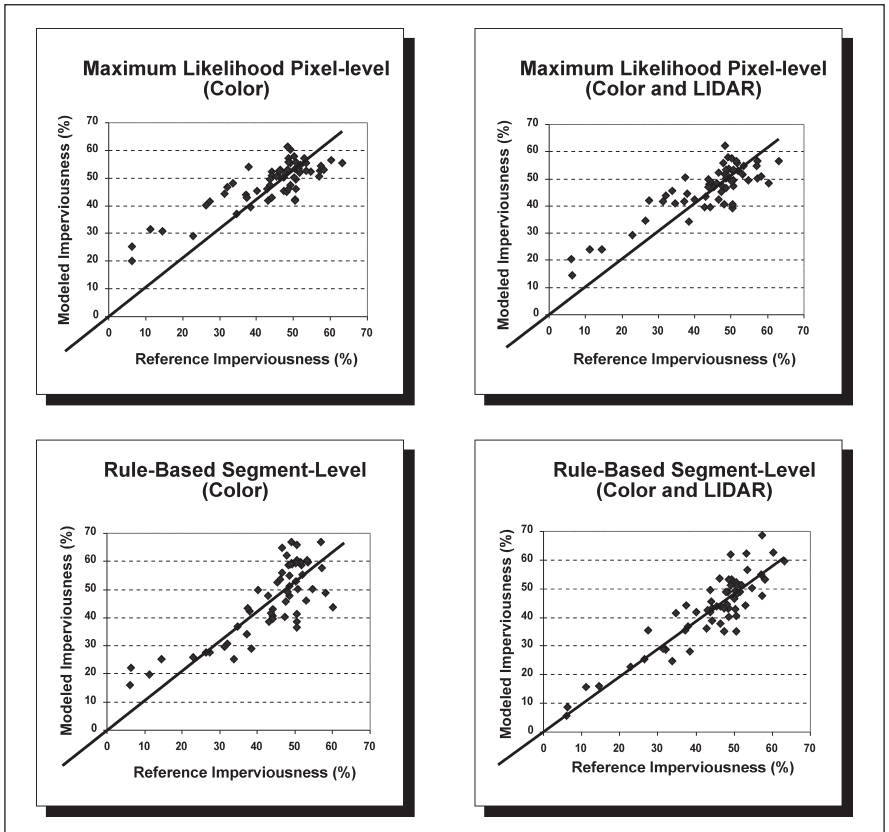

Figure 3. Scatter plots between modeled percent imperviousness and reference percent imperviousness. Regression lines are shown. The maximum-likelihood *per-pixel* classifications and See5 rule-based *per-segment* classifications are shown.

imperviousness (thin- and thick-forested parcels), the addition of cover height resulted in a considerable improvement in imperviousness estimates. For the maximum-likelihood classification, the addition of cover height had little effect on the accuracy for the more impervious parcels (e.g., residential and commercial). The addition of cover height using the rule-based classifier with segments resulted in a much better linear relationship between modeled imperviousness and reference data.

Model Performance

The two best imperviousness surface models were derived using the *maximum-likelihood per-pixel* classification and the *rule-based per-segment* classification (Table 1). The regression slope for all models was significantly different from 0.0 at the 0.01 probability level. The rule-based per-segment algorithm and the maximum-likelihood per-pixel algorithm explained 78 percent and 71 percent of the variance in imperviousness,

respectively. Using the combined color imagery and lidar-derived cover height, modeled imperviousness for all parcels was within 15 percent of reference imperviousness. The standard error for the rule-based *per-segment* model was only 5.85 percent. Maximum observed error was only 14.85 percent. For the *per-pixel* classification using the maximum-likelihood algorithm the standard error was 6.62 percent and maximum error was 14.16 percent. Thus, these two models were both acceptable for predicting parcel-level imperviousness.

The *rule-based pixel-level* classification approach provided moderately good results. Standard errors were slightly higher (i.e., from 7.15 to 9.06) than the maximum-likelihood per-pixel or rule-based per-segment classifications. However, the regression line slopes were considerably different from 1.0 (i.e., 0.695, 0.709, 1.650). Also, the maximum errors ranged from −17 percent to −27 percent.

The *ISODATA clustering pixel-level* classification approach did not perform well. The R^2 values were the lowest, the standard errors were the highest, and the maximum errors were the highest of all models.

All classification models tended to overpredict imperviousness where reference imperviousness was low (0 to 30 percent imperviousness). The maximum-likelihood classification model consistently overpredicted imperviousness in the low range (Figure 3). These overpredicted residuals are positive in this range. The dominant cause of overprediction in this low imperviousness range was the misclassifiation of shadows as water. However, the maximum residuals for most models were negative (Table 1), indicating an overall underprediction in imperviousness.

Level-of-Effort

The goal was to find an accurate and *efficient* method for the Richland County Public Works Department to inventory impervious surfaces throughout an entire county. Therefore, it was important to estimate the level-of-effort required for such an endeavor. Creation of the image segments required about 2 hours. Selection of the training areas required about 1 hour of manual effort. The data were processed using a dual Xeon (1.8 gHz) workstation with 1 gb of main memory. The same machine was used to generate the production rules using the See5 algorithm in the rule-based classification scenarios. Generation of the rules for the pixel-level classification of the color and combined color/height data required 4.4 hours and 5.4 hours, respectively. Generation of the rules for the per-segment classification was negligible. It is noted that processing time for generating rules increases exponentially with the number of training observations. Total classification times (Table 2) for the pixel-level approaches ranged in time from 0.3 hours (maximum-likelihood) to 9 hours (rule generation and inference combined).

The study area (19.8 km^2) represented approximately one percent of the total land area of Richland County (2,000 km^2).

TABLE 2. CLASSIFICATION TIME REQUIREMENTS*

Approach	Color Imagery	Lidar Height	Color Imagery and Cover Height
Per-Pixel			
Maximum-Likelihood	0.2 h	0.2 h	0.3 h
ISODATA	1.7 h	1.1 h	1.7 h
See5 Rule-Based	8.0 h	0.25 h	9.0 h
Per-Segment			
See5 Rule-Based	negligible	negligible	negligible

*ISODATA times include the manual labeling of clusters.

The 60 parcels studied were composed of 1,002,148 pixels (0.3- by 0.3-m pixels) or 497 image segments. In order to use this approach across the entire County of Richland, a minimum of 30 hours for the maximum-likelihood method is required. For the rule-based pixel-level approach, approximately 1,000 hours (42 days) is required. This amount of time for a rule-based pixel-level classification may not be feasible for an applied project, even if the resulting accuracies are slightly higher. The use of a per-segment analysis with a rule-based classifier may be appropriate. The per-segment classification approach would require additional computation time and format conversion for image segmentation (estimate of 15 hours).

Summary

This study evaluated the relative contribution of lidar-derived cover-height information coupled with digitized high spatial resolution color orthophotography for mapping urban parcel imperviousness. In all analyses, the cover-height information resulted in an improved imperviousness product. The best approaches were (1) per-pixel maximum-likelihood classification and (2) per-segment See5 rule-based classification. For these two approaches, the maximum error in parcel-level imperviousness was less than 15 percent while the standard error was approximately 6 percent. The 15 percent error at the parcel level was comparable to the 10 percent error found in the Wu and Murray (2002) and Ji and Jensen (1999) studies.

Similar to Wu and Murray's (2002) model for impervious surface estimation, we also found using the maximum-likelihood per-pixel classifier a slight *over*estimation of imperviousness when the percentage imperviousness was low (e.g., in less-developed areas). The rule-based per-segment classifier was nearly perfect in predicting imperviousness for parcels with low imperviousness. Wu and Murray's (2002) model also underestimated imperviousness at the other extreme (in highly urbanized areas). Ji and Jensen's sub-pixel approach (1999), slightly *under*predicted imperviousness.

Although a relatively low overall error was noted in this research, there are several things that can be done to further improve impervious surface classification. One of the notable problems in classifying the high-resolution imagery was the misclassification of pixels containing shadows. Typically, the low reflectance from pixels under shadow results in a misclassification into the water class. For residential environments, these "shadowed" pixels are likely either grass, landscaped, or surfaced areas. Thus, the actual imperviousness is from 20 to 60 percent versus the classified imperviousness of water—100 percent. In commercial environments, the shadowed pixels (near buildings) are often paved areas and thus result in negligible impervious surface errors. The net effect of classifying shadowed areas as water is to overpredict percent imperviousness (Figure 3). A major improvement in the classification approach would be to develop a method for accurately estimating the land cover in shadow. Unfortunately, this problem requires first accurately determining what pixels are under shadow before estimating the shadowed land cover. Previous research has offered some approaches for this problem (Hodgson *et al.*, 1988; Gilabert *et al.*, 2000). The addition of a near-infrared band would be helpful in discriminating between shadowed and water land cover.

In addition, inherent in high-resolution imagery is the variation in features that one would expect to be constant. For example, when using lower resolution imagery, a roof is a roof, but when using high resolution imagery, there is variation between the different pitches (both in slope and aspect) and different materials (Plate 1c). This makes the discrimination into a single class difficult. Spatial operators (e.g., texture, neighborhood complexity, etc.) were not investigated in this study but may result in an improved product.

Either of the two "best" approaches may be acceptable for countywide mapping of surface imperviousness at the parcel level. The rule-based segment classifier produced a slightly superior product than did the maximum-likelihood pixel-level classifier (R^2 of 0.78 versus 0.61, respectively). Segment-based classification requires a segment extraction algorithm (e.g., the eCognition software), a rule-generation package (e.g., See5), and a minor amount of computing resources to classify the image. In addition, the per-segment or rule-based classification approach may be somewhat new to the GIS/remote sensing staff at local agencies. The adoption of either method would produce acceptable results and the selection should be based on the available expertise and resources.

Acknowledgments

This research was funded, in part, by NASA's Affiliated Research Center program at the Stennis Space Center, Mississippi. The Richland County Information Technology Department provided the digital orthophotography and lidar data used in this effort. We are grateful to Bruce Davis at NASA and Patrick Bresnahan at Richland County for their contributions.

References

Civco, D.L., J.D. Hurd, C.L. Arnold, S. Prisloe, 2000. Characterization of suburban sprawl and forest fragmentation through remote sensing applications, *Proceedings of the ASPRS 2000 Annual Convention*, 22–26 May, Washington, D.C. (American Society for Photogrammetry and Remote Sensing, Bethesda, Maryland), unpaginated CD-ROM.

Clark, W.A.V. and K.L. Avery, 1976. The effects of data aggregation in statistical analysis, *Geographical Analysis*, 8:428–438.

Definiens, 2002. *eCognition 2.1 User Guide* (object oriented image classification software), Definiens Imaging GmbH, München, Germany, 417 p.

Fankhauser, R., 1999. Automatic determination of imperviousness in urban areas from digital orthophotos, *Water Science and Technology*, 39(9):81–86.

Gilabert, M.A., F.J. Garcia-Haro, and J. Melia, 2000. A mixture modeling approach to estimate vegetation parameters for heterogeneous canopies in remote sensing, *Remote Sensing of Environment*, 72:328–345.

Hodgson, M.E., 1998. What size window for image classification?—A cognitive perspective, *Photogrammetric Engineering & Remote Sensing*, 64(8):797–808.

Hodgson, M.E., J.R. Jensen, J. Pinder, and H.E. Mackey, 1988. Vegetation mapping using high resolution MSS data: Canopy reflectance and shadow problems encountered and possible solutions, *Proceedings of the ASPRS 1998 Annual Convention*, 13–18 March, St. Louis, Missouri (American Society for Photogrammetry and Remote Sensing, Bethesda, Maryland), pp. 32–39.

Hodgson, M.E. and P. Bresnahan, in press. Accuracy of airborne lidar derived elevation: empirical assessment and error budget, *Photogrammetric Engineering & Remote Sensing*.

Huang, X., and J.R. Jensen, 1997. A machine-learning approach to automated knowledge-base building for remote sensing image analysis with GIS data, *Photogrammetric Engineering & Remote Sensing*, 63(10):1185–1194.

Ji, M., and J.R. Jensen, 1999. Effectiveness of subpixel analysis in detecting and quantifying urban imperviousness from Landsat Thematic Mapper imagery, *Geocarto International*, 14(4):31–39.

Kienegger, E.H., 1992. Assessment of a wastewater service charge by integrating aerial photography and GIS, *Photogrammetric Engineering & Remote Sensing*, 58(11):1601–1606.

Lloyd, R.E., M.E. Hodgson, and A. Stokes, 2002. Visual categorization with aerial photographs, *Annals of the Association of American Geographers*, 92(2):241–266.

Lohani, V., D.F. Kibler, and J. Chanat, 2002. Constructing a problem solving environment tool for hydrologic assessment of land use change, *Journal of the American Water Resources Association*, 38(2):439–452.

Paul, M.J., and J.L. Meyer, 2001. Streams in the urban landscape, *Annual Review Ecological Systems*, 32:333–365.

Phinn, S., M. Stanford, P. Scarth, A.T. Murray, and P.T. Shey, 2002. Monitoring the composition of urban environments based on the vegetation-impervious surface-soil (VIS) model by subpixel analysis techniques, *International Journal of Remote Sensing*, 23(20):4131–4153.

Quinlan, J.R., 1993. *C4.5: Programs for Machine Learning*, Morgan Kaufman Publishers, San Mateo, California, 302 p.

Ridd, M.K., 1995. Exploring a V-I-S (vegetation-impervious surface-soil) model for urban ecosystem analysis through remote-sensing—Comparative anatomy for cities, *International Journal of Remote Sensing*, 16(12):2165–2185.

RuleQuest Research, 2001. *See5 Release 1.13* (data mining software), RuleQuest Research, St. Ives NSW, Australia.

Sleavin, W.J., D.L. Civco, S. Prisloe, and L. Giannotti, 2000. Measuring impervious surfaces for non-point source pollution modeling, *Proceedings of the ASPRS 2000 Annual Convention*, 22–26 May, Washington, D.C. (American Society for Photogrammetry and Remote Sensing, Bethesda, Maryland), unpaginated CD-ROM.

Stow, D., L. Coulter, J. Kaiser, A. Hope, D. Service, K. Schutte, and A. Walters, 2003. Irrigated vegetation assessment for urban environments, *Photogrammetric Engineering & Remote Sensing* 69(4):381–390.

Tullis, J.A., and J.R. Jensen, 2003. Expert system house detection in high spatial resolution imagery using size, shape, and context, *Geocarto International*, 18(1):5–15.

Warwick, J.J., and P. Tadepalli, 1991. Efficacy of SWMM application, *Journal of Water Resources Planning and Management*, 117(3):352–366.

Wu, C.S., and A.T. Murray, 2003. Estimating impervious surface distribution by spectral mixture analysis, *Remote Sensing of Environment*, 84(4):493–505.

Zug, M., L. Phan, D. Bellefleur, and O. Scrivener, 1999. Pollution wash-off modeling on impervious surfaces: Calibration, validation, transposition, *Water Science and Technology*, 39(2):17–24.